Journal of Functional Foods 56 (2019) 232–245

Contents lists available at ScienceDirect

Journal of Functional Foods

journal homepage: www.elsevier.com/locate/jff

A probiotic formulation containing *Lactobacillus bulgaricus* DWT1 inhibits tumor growth by activating pro-inflammatory responses in macrophages

Dipanjan Guha[a,1], Arka Banerjee[a,2], Raktim Mukherjee[a], Biswaranjan Pradhan[a,3], Maria Peneva[b], Georgi Aleksandrov[b], Sujit Suklabaidya[c], Shantibhushan Senapati[c], Palok Aich[a,*]

[a] *School of Biological Sciences, National Institute of Science Education and Research (NISER), HBNI, P.O. - Bhimpur-Padanpur, Jatni – 752050, Dist. -Khurdha, Odisha, India*

[b] *Daflorn Ltd., St. Ivan Rilski Str., No. 10, Sofia 1606, Bulgaria*

[c] *Institute of Life Sciences, Nalco Square, Chandrasekharpur, Bhubaneswar, Odisha 751023, India*

ARTICLE INFO

Keywords:
Lactobacillus delbruckei sp. *Bulgaricus* DWT1
Macrophage polarization
In vitro
In vivo
Tumor
Probiotic

ABSTRACT

Probiotics are functional foods and are becoming more evident with time that probiotics can have prophylactic and therapeutic roles. Current report revealed that an established probiotic cocktail of *Lactobacillus delbruckei* sp. *bulgaricus* DWT1 and *Streptococcus thermophilus* DWT4, could inhibit tumor growth. This probiotic cocktail is already marketed in various forms of food supplement. Present report reveals the transition of M2 to M1 like state of macrophage cells of mouse origin *in vitro, ex vivo* and *in vivo* following treatment with the established probiotic cocktail. Current study for the first time suggests the ability of a probiotic formulation to polarize macrophages from M2 to M1 state with potentials of developing newer intervention strategies for tumor growth. As a validation of our claim, we have established a novel and significant way of tumor inhibition in mouse model by the probiotic formulation that is capable of polarizing macrophages from M2 to M1.

1. Introduction

Finding a cure and that too intrinsic for cancer therapy is a challenge but may not be impossible. Answer may be hidden in the efficacy of certain bacteria known as probiotics or functional foods. One of the biggest challenges in modern science is to develop an effective methodology to inhibit tumor growth. Chemotherapy (Van Cutsem et al., 2009) and radiation therapy (Milenic, Brady, & Brechbiel, 2004) are, by far, the best ways to cease tumor growth, but they have multiple limitations (Dean, Fojo, & Bates, 2005; Knox & Meredith, 2000). In this context, finding an intrinsic way to inhibit tumor growth is one of the biggest challenges. Polarization of tumor associated macrophage (TAM) plays an important role to control tumor growth intrinsically (Mantovani, Allavena, Sica, & Balkwill, 2008). Activated macrophages exist mainly in two polarized states: pro-inflammatory (M1) and anti-inflammatory (M2) (Mosser & Edwards, 2008).

Anti-inflammatory macrophages are instrumental for tumor growth, helping the tumor to undertake angiogenesis, supply of various growth factor, down-regulating adaptive immune system, and modulating extracellular matrix for metastasis and proliferation (Chanmee, Ontong, Konno, & Itano, 2014; Vinogradov, Warren, & Wei, 2014). Anti-inflammatory polarized macrophages, otherwise known as alternatively activated macrophages or M2 (Martinez & Gordon, 2014) are characterized by increased phagocytic and scavenging activity (Reid, Jass, Sebulsky, & McCormick, 2003) and polyamine/ornithine synthesis by the arginase pathway (Wang, Liang, & Zen, 2014). Anti-inflammatory expression of IL4 and IL10 is high and that of IL12 is low (Gordon, 2003; Mantovani, Sozzani, Locati, Allavena, & Sica, 2002). Role of the anti-inflammatory activation state is, therefore, tolerogenic (Mantovani, Biswas, Galdiero, Sica, & Locati, 2011).

While the anti-tumor activity of pro-inflammatory macrophages is well reported. Pro-inflammatory macrophages can recognize cancer cells, destroying those by phagocytosis (Lamagna, Aurrand-Lions, & Imhof, 2006; Solinas, Germano, Mantovani, & Allavena, 2009). Recent report showed, iron nanoparticle (Zanganeh et al., 2016) and genetically engineered *Salmonella typhimurium* (Zheng et al., 2017) has been

* Corresponding author.
E-mail address: palok.aich@niser.ac.in (P. Aich).
[1] Present address: University of Kalyani, Kalyani, West Bengal, India.
[2] Present address: Biozentrum der Universität Basel, 50-70 Klingelbergstrasse, 4056 Basel, Switzerland.
[3] Present address: S. K. Dash Center of Excellence of Biosciences and Engineering & Technology (SKBET), Indian Institute of Technology Bhubaneswar, Odisha, India.

https://doi.org/10.1016/j.jff.2019.03.030
Received 10 December 2018; Received in revised form 12 March 2019; Accepted 18 March 2019

used to put the TAM in pro-inflammatory state, showing an inhibition in tumor growth *in vivo*. Pro-inflammatory polarized macrophages are also known as classically activated macrophages or M1 (Martinez & Gordon, 2014). Classically activated macrophages are characterized by high expression of pro-inflammatory cytokines such as IL1, IL6, IL8, TNF and IFNγ (Dinarello, 2000; Lyke et al., 2004), increased production of reactive nitrogen and oxygen species. Hence, the purpose of pro-inflammatory activation of a macrophage is to control and suppress an infection by creating a pro-inflammatory environment (Lawrence & Natoli, 2011).

Transition, from M1 to M2 polarized states of macrophages, has been well studied in association with endotoxin tolerance. Little is, however, known about the transition from anti-inflammatory (M2) to pro-inflammatory (M1) macrophages. In the current study, we are reporting for the first time that probiotic-induced activation of transition from anti-inflammatory like macrophages to pro-inflammatory like state. In the present report, we validated the effects of *Lactobacillus delbruckei* sp. *bulgaricus* strain DWT1; CCM 7992 (LDB) and *Streptococcus thermophilus* strain DWT4; CCM 7992(ST), an established probiotic cocktail (LDB-ST), on transition of M2 polarized state of a) murine macrophage cell line RAW 264.7 (*in vitro*), b) peritoneal macrophages (*ex vivo*) and c) TAM (*in vivo*). Qualitatively it is well known that ST, an established bacteria to make yogurt, is functional in benefiting and maintaining health along with proto-cooperative bacteria LDB (Herve-Jimenez et al., 2009). LDB and ST are in a cooperative relation where the presence of ST stimulates the growth of LDB by producing formic acid and carbon dioxide, while LDB assists ST growth by providing necessary amino acids via protein degradation (Driessen, Kingma, & Stadhouders, 1982; Veringa, Galesloo, & Davelaar, 1968). It has been reported that LDB along with ST is effective and functional formulation to elicit effects *in vivo* and clinically active against pathogens (Carper, 1994). Current study established the effects of probiotic cocktail of LDB and ST on macrophage polarization *in vitro, ex vivo* and *in vivo*, which led us, to look for translational application of the probiotic cocktail. LDB-ST, showing such consistent time dependent anti-inflammatory to pro-inflammatory polarization of macrophages, is an appropriate candidate to study tumor inhibition, without the cytotoxic effect on macrophages. The application of the said probiotic mixture to a pancreatic cancer model was tested. We observed significant reduction in the orthotopic tumor load in the treated mice compared to the untreated one. This study opens up potential novel avenues using macrophage polarization following treatment with probiotics and newer approaches for cancer treatment by manipulating tumor-associated macrophages to express pro-inflammatory genes.

2. Materials and methods

2.1. Animal cell culture

The murine macrophage cell line, RAW 264.7 (National Centre for Cell Science, Pune, India) was routinely cultured in our laboratory. Cells were grown in RPMI-1640 medium (Himedia, India) supplemented with 10% heat inactivated fetal bovine serum (Himedia, India) (without any antibiotic) in 75 cm^2 tissue culture flasks (BD Biosciences, USA) at 37 °C in a humidified atmosphere containing 5% CO_2. The cells were sub-cultured twice a week to maintain an exponential growth rate. After reaching 70% confluency, cells were washed with Dulbecco's phosphate buffered saline (PBS) and trypsinized with 0.25% trypsin solution containing 0.001% EDTA (Himedia, India) and re-plated for growth (Pradhan, Guha, Ray, Das, & Aich, 2016).

2.2. Bacterial cell culture

LDB-ST was a gift from Daflorn Ltd. (Sofia, Bulgaria). LDB-ST grows well in MRS broth (Himedia, India). LDB-ST from glycerol stock of 100 µl was added in 20 ml of MRS broth and kept in a shaker incubator (Innova42, New Brunswick Scientific, Germany) for 4 h at 37 °C (200 rpm) to make the desired bacterial culture. O.D. at 600 nm was measured to determine the bacterial density inside culture medium.

2.3. In vitro treatment

RAW 264.7 cells were treated with LDB-ST (growing in log phase) for 1 h at required MOI(s) in antibiotic free RPMI-1640 supplemented with 10% FBS. Media was aspirated and cells were washed thrice with PBS to remove free bacteria. Fresh antibiotic free media was then added to the cells. For experimental analysis, cells were then collected by trypsinization following desired time of incubation. Time matched control cells were handled similarly, but without bacterial treatment.

2.4. Cell viability assay by trypan blue dye exclusion method

1×10^6 RAW 264.7 cells were grown in antibiotic-free culture media in 6 well plates. Following 16 h of stabilization, cells were treated with probiotics LDB-ST (grown to log phase) was treated at MOI 0.5, 1, 10 and 100. For each of the time points, a set of untreated cell was kept as control. Cells were trypsinized and collected at 1, 2, 4 and 6 h post treatment and counted following staining with 0.2% trypan blue (Himedia, India). Cells were treated with *Salmonella typhimurium* serovar *enterica* MTCC-3232 (ST′) at MOI of 10 as a positive control to check the cytotoxicity of the bacteria. The percentage survival was calculated using the formula given below:

$$\text{Percentage survivality} = (\text{No. of live cells/No. of cells plated}) * 100.$$

The assays were done with three biological replicates.

2.5. RNA isolation and quality control

After required treatment, cells were harvested and washed twice with PBS. RNA was extracted using RNeasy mini kit (Qiagen, Germany) as per manufacturer's protocol. To summarize the protocol, cells were gently lysed with 350 µl RLT buffer, and then homogenized using QIA shreadder (Qiagen, Germany). Equal volume of 70% ethanol was added to the homogenate, mixed by pipetting and passed through the RNeasy mini column, which retains the RNA in a silica matrix. The column was then washed once with 750 µl RW1 buffer and twice with 500 µl RPE buffer to remove unwanted lipid, protein and DNA from the matrix. RNA was then eluted from the matrix with 30 µl nuclease free water and kept on ice.

RNA quantification and quality were done spectro-photometrically using Nanodrop2000 (Thermo Scientific, USA). RNA integrity was checked using a bioanalyzer2100 (Agilent, USA) using RNA 6000 Nano kit (Agilent, USA) as per the manufacturer's protocol. RNA integrity of a value 8.5 or higher was considered for downstream applications such as quantitative real time polymerase chain reaction (qRT-PCR) and gene expression microarray.

2.6. cDNA synthesis

cDNA was synthesized from RNA using AffinityScript One-Step RT-PCR Kit (Agilent, USA). cDNA synthesis were done using the protocol described by Pradhan et al. (2016). Briefly, 5 µg of total RNA was mixed with the buffer containing affinityscript reverse transcriptase and polyT primer. The mixture was kept in the thermo cycler at 45 °C for 30 min to synthesize c-DNA. Then the temperature was raised to 92 °C for 1 min to deactivate the enzyme.

2.7. Microarray

The RNA samples for gene expression were labeled using Agilent Quick-Amp labeling Kit (p/n5190-0444 Agilent, USA). Sample preparation for microarray was done following the protocol used by Pradhan et al (Pradhan et al., 2016). RNA samples from control and treated cells (500 ng each) were incubated with reverse transcription mix at 40 °C and converted to c-DNA primed by oligodT with a T7 promoter. Synthesized c-DNA was used as template for c-RNA generation. c-RNA was generated by *in vitro* transcription and the dyes Cy3 CTP (control sample) and Cy5 CTP (treated samples) was incorporated to c-RNA during this step. The c-DNA synthesis and *in vitro* transcription steps were carried out at 40 °C. Labeled c-RNA was cleaned up and quality assessed for yields and specific activity. The labeled c-RNA samples were hybridized to 4x44k microarray slides. 825 ng each of Cy3 and Cy5 labeled samples were fragmented and hybridized. Fragmentation of labeled c-RNA and hybridization were done using the Gene Expression Hybridization kit (Part Number 5188–5242, Agilent, USA). Hybridization was carried out in Agilent's Surehybrid Chambers at 65 °C for 17 h in humidified condition. The hybridized slides were washed using Agilent Gene Expression wash buffers (Part Number 5188–5327, Agilent, USA). The image of the microarray slides was taken immediately on a microarray scanner (Agilent Sure Scan-C) using the Agilent scan control software. Data extraction from images was done using Feature Extraction software Version 10.7 (Agilent, USA). Those data were analyzed in array-pipe (v2.0). The differentially expressed genes were filtered based on p-value (< 0.05) and fold changes (> 1.5). Differentially regulated unique as well as common genes at different conditions were segregated by Venn diagram, generated using free web based software "Bioinformatics & Evolutionary Genomics" (http://bioinformatics.psb.ugent.be/webtools/Venn/). Those differentially regulated genes are clustered in pathways using WEB-based Gene SeT AnaLysis Toolkit (Webgestalt). Pathway analysis was done using KEGG PATHWAY Database.

2.8. qRT-PCR assay

qRT-PCR reaction was set-up in 96 well PCR plates. The template, required primer (sequence of primers are listed in Table 1), buffer and SYBR green along with DNA polymerase were added in a PCR plate as per the manufacturer's (Promega, USA) protocol. The plate was then kept in the qRT-PCR machine (Mx3005P, Stratagene, USA) and the machine was programmed as follows; 2 min at 92 °C to activate DNA polymerase for 1 cycle, 15 sec at 92 °C for melting and 1 min at 60 °C for primer annealing along with extension of the chain and detection of the florescence for 40 cycles. Cycle threshold (Ct) values were noted, and fold changes of the desired genes were calculated, with respect to the control after normalizing with internal control gene, β-actin. The qRT-PCR is done with three technical replicates along with no template control and no primer control. The kinetics of few selected genes was checked through qRT-PCR.

2.9. Enzyme-linked immunosorbent assay (ELISA)

Supernatants from control and treated cells were used to measure the level of secreted TNFα, IL1b, IL6, IL12 and TGFβ by ELISA. Experiments were conducted using the protocol used by Xie, Ortega, Mora, and Chapes (2010). Briefly, the ELISA plates were coated with supernatant overnight at 4 °C. Following 1 h of blocking, antibodies were added to each well and were incubated at 4 °C for 6 h. Wells were washed three times with PBS supplemented with 0.5% Tween 20 (PBST). Biotin-conjugated detection antibodies were added and incubated at 4 °C for 2 h. Alkaline phosphatase-conjugated streptavidin was then added and incubated at room temperature for 1 h. After three washes, the substrate was added to the wells. Within 45 min, the reaction was stopped by the addition of 50 µl of 1 N H_2SO_4, and absorbance was assessed using a Bio-Rad microplate reader, model 680 (Bio-Rad Laboratories, USA) at 450 nm. Fold change was calculated using the formula given below:

$$\text{Fold change} = (OD^{\text{Treated}} - OD^{\text{Control}})/OD^{\text{Control}}$$

The assays were done with three technical replicates.

2.10. Fluorescence microscopy

RAW 264.7 cells were seeded on a glass cover-slip placed in a 6 well

Table 1
List of primers used for qRT-PCR.

Gene name	Forward Primer	Reverse Primer	NCBI Sequence Accession number
Il1b	5′-TTGAAGAAGAGCCCATCCTCTGTG-3′	5′-TGTGAGGTGCTGATGTACCAGTTG-3′	NM_008361.3
Il6	5′-AGACAAAGCCAGAGTCCTTCAGAG-3′	5′-CCACAGTGAGGAATGTCCACAAAC-3′	NM_031168.1
Il10	5′-TGGGAGGGGTTCTTCCTTGG-3′	5′-GGGAACCCTCTGAGCTGCTG-3′	NM_010548.2
Il12	5′-CGCCCAAGAACTTGCAGATGAAGC-3′	5′-CGCCTTTGCATTGGACTTCGGTAG-3′	NM_001303244.1
Tgfβr1	5′-TGGCAGTGGAAGTTGGCCTCAG-3′	5′-GGGCCTCAAGGCACTTCTGGAG-3′	NM_009370.3
Arg1	5′-GATTGGCAAGGTGATGGAAGAGAC-3′	5′-TCTGTAAGATAGGCCTCCCAGAAC-3′	NM_007482.3
Nos2	5′-GCAACTACTGCTGGTGGTGACAAG-3′	5′-GGAAGTGAAGCGTTTCGGGATCTG-3′	NM_001313922.1
Tnfr	5′-ATAAAGCCACACCCACAACC-3′	5′-GACCTTTGCCCACTTTTCAC-3′	NM_011609.4
Fadd	5′-GCGCCGACACGATCTACTG-3′	5′-TTACCCGCTCACTCAGACTTC-3′	NM_010175.5
Casp8	5′-TGCTTGGACTACATCCCACAC-3′	5′-TGCAGTCTAGGAAGTTGACCA-3′	NM_001277926.1
Casp3	5′-TGGTGATGAAGGGGTCATTTATG-3′	5′-TTCGGCTTTCCAGTCAGACTC-3′	NM_009810.3
Casp7	5′-CGGAATGGGACGGACAAAGAT-3′	5′-CTTTCCCGTAAATCAGGTCCT-3′	NM_007611.2
Bid	5′-CCATGTAGGTGGGCTTCTGT-3′	5′-GATCAGCCATTCGGCTTTTA-3′	NM_007544.3
Bcl2	5′-ATGCCTTTGTGGAACTATATGGC-3′	5′-GGTATGCACCCAGAGTGATGC-3′	NM_009741.5
Bax	5′-TGAAGACAGGGGCCTTTTTG-3′	5′-AATTCGCCGGAGACACTCG-3′	NM_007527.3
Cytc	5′-CCAAATCTCCACGGTCTGTTC-3′	5′-ATCAGGGTATCCTCTCCCCAG-3′	NM_007808.4
Apaf1	5′-GCCAATGTGATGGGTGAAAC-3′	5′-TGACGGTTGCTGTTCACTTC-3′	NM_009684.2
Casp9	5′-TCCTGGTACATCGAGACCTTG-3′	5′-AAGTCCCTTTCGCAGAAACAG-3′	NM_015733.5
Tlr1	5′-GTGCCCGTCCCAAGTTAGCC-3′	5′-GTCCAGGCGCATGGGATTC-3′	AY009154.1
Tlr2	5′-GCCCGTAGATGAAGTCAGCTCACC-3′	5′-GCCCGTAGATGAAGTCAGCTCACC-3′	NM_011905.3
Rac1	5′-CGAAGCTATCCGAGCGGTTCTCTG-3′	5′-CACACGGTCTGGGAACTCTGGAAG-3′	NM_009007.2
Pi3kca	5′-GGGCTGGACCCCCACACTAC-3′	5′-TCTCCCTGCTCAGGCCCTTC-3′	NM_008839.2
Akt1	5′-CAAGGACGGGCACATCAAGATAAC-3′	5′-TGGGCTCAGCTTCTTCTCATACAC-3′	NM_001165894.1
Nfkb1	5′-CAGGGTATGGCTACTCGAACTACG-3′	5′-CCAGATGTGACTTCCAGCAGATCC-3′	NM_008689.2
Ikb	5′-AGCGAGCAGCCATGATGAGTCTCC-3′	5′-ATTGCCTGAAGCAGCAGCCGTACC-3′	NM_001159774.1
Tnf	5′-CCCACGTCGTAGCAAACCACCAAG-3′	5′-TGCCCGGACTCCGCAAAGTCTAAG-3′	NM_013693.2
β-actin	5′-CTGACGGCCAGGTCATCACTATTG-3′	5′-GACAGCACTGTGTTGGCATAGAGG-3′	NM_007393.3

plate for fluorescence microscopy. Following desired treatment (i.e. RAW 264.7 cells were treated with LDB-ST at MOI of 10 for 1 and 6 h; as a positive control for pro-inflammatory macrophages, RAW 264.7 cells were treated with LPS (Sigma, USA) at a concentration of 1 μg/ml for 24 h), cells were fixed with PFA for 30 min. After thoroughly washing with PBS, cells were treated with 0.25% Triton X-100 (in PBS) for 10 min for permeabilization. To avoid unwanted antibody binding, cells were kept in blocking solution (contains 1% BSA in PBST (PBS + 0.1% Tween 20)) for 1 h at 4 °C. Following washing with PBS, cells were stained by with Dylight 488 (Abcam, UK) conjugated anti-iNOS antibody (Abcam, UK) and anti-ARG antibody (Abcam, UK) at a concentration of 5 μg/ml at 4 °C. After 2 h, cells were washed to remove the un-bound antibody and then stained with hoechst (Himedia, India) at a concentration of 2 μg/ml. The coverslip (containing cells) was then washed with PBS and mounted on a glass slide with fluormount G (Sigma, USA) under moist condition. The glass slide was kept at room temperature and in the dark for 6 to 12 h to ensure proper mounting. Microscopy was done using fluorescence microscope (Carl Zeiss, Germany).

2.11. Flow cytometry

We assayed pan-macrophage marker CD68 and macrophage cell surface marker CD11c and CD206 in cells by BD FACS Calibur (BD, USA) and BD LSR Fortessa (BD, USA). Antibody staining for flow cytometry were done using the protocol described by Guha, Bhowmik, and Ghosh (2014). Briefly, following desired treatment cells were suspended in PBS. Suspension was incubated with a blocking solution containing 1% BSA and 0.1% Triton X-100, for 10 min at room temperature. Excess blocking solution was washed with PBS by centrifugation at 2500 rpm for 5 min at room temperature. The cell pellet was further washed with PBS and re-suspended in 100 μl of PBS. Next, 1 μg of primary antibodies (Abcam, UK) were added to each tube, vortexed gently, and incubated for 30 min in a covered ice bucket. Excess antibody was washed with PBS by centrifugation for 5 min at 2500 rpm, 4 °C. Without disturbing the pellet, PBS was aspirated out. Then, the cells were re-suspended in blocking solution at 4 °C. After 10 min, cells were washed with PBS by centrifugation for 5 min at 2500 rpm, 4 °C. The pellet was again suspended in 100 μl of PBS; 1 μg of fluorochrome conjugated secondary antibody (Abcam, UK) was added, which was then gently vortexed and incubated for 30 min in a covered ice bucket. To wash off excess antibody, PBS was added to each tube and centrifuged for 5 min at 2500 rpm, 4 °C. The supernatant was aspirated out gently. Pellet was re-suspended in 500 μl of PBS. Fluorescence-conjugated antibody on cells was measured by flow-cytometer.

2.12. Peritoneal macrophage extraction and treatment ex vivo

The peritoneal cavity cells were extracted from mice according to the protocol described by Ray and Dittel (2010). All experiments involving mice were approved by the Institute Animal Ethics committee of NISER as per the guidelines of CPCSEA (Committee for the Purpose of Control And Supervision of Experiments on Animals). We obtained, on average, 5×10^5 cells per mouse. We used total of 60 mice for this study. Following extraction, peritoneal macrophages were maintained in RPMI-1640 medium (Himedia, India) supplemented with 10% heat inactivated fetal bovine serum (Himedia, India), without any antibiotic, in 75 cm^2 tissue culture flasksat 37 °C in a humidified atmosphere containing 5% CO_2 for 6 h for plastic surface adherence of the macrophage cells. Non-macrophage cells were removed by washing with ice-cold PBS thrice for 30 sec each. The cells were maintained and treated with the probiotic using same protocol as described for treatment *in vitro*. The cells were used for RNA extraction and for further analysis.

2.13. In vivo treatment (Intra-Peritoneal injection) and peritoneal cell collection

BALB/c and C57BL/6 mice of 6 weeks of age were divided into groups (n = 3) of control and treatment. Treatment group consists of mice that were treated with cocktail formulation of LDB and ST. The probiotics were grown to log phase and LDB-ST was injected intraperitoneal with 250 μl of saline water at the dose of 5×10^5 CFU to the mice at hour zero. Health of mice then followed for any abnormal behavior observed. The treated mice were sacrificed on 4, 6, 8 and 12 h post treatment and peritoneal cells were collected by the previously mentioned protocol. The cells were used for RNA extraction and for further analysis.

2.14. Oral treatment and tissue collection

BALB/c and C57BL/6 mice of 6 weeks of age were divided into groups (n = 3) of control and treatment. LDB-ST was orally gavaged with 250 μl of saline water at the c.f.u. of 1×10^9 to the mice on day zero. The treated mice were sacrificed on day 1, 3, 5 and 7 and tissue samples were collected from ileum and colon. The tissue samples were stored in RNA later (Sigma, USA) for RNA extraction and analysis.

2.15. Trans-well co-culture of C57BL/6 peritoneal macrophage and UN-KC-6141 cells

C57BL/6 mice of 6 weeks' age were used for collection of peritoneal macrophage using the protocol described above. These cells were seeded inside trans-well inserts at 5×10^5cells per insert. The wells were seeded with 10^6 UN-KC-6141 cells. UN-KC-6141 cells are pancreatic tumor cell line from mouse (Torres et al., 2013). The UN-KC-6141 cell line was a generous gift from Dr. Surinder K. Batra (University of Nebraska Medical Centre, USA) to Senapati lab at the Institute of life sciences, Bhubaneswar.

The cells were cultured independently. The peritoneal macrophages were treated with LDB-ST by the previously mentioned protocol. The trans-well inserts were shifted into co-culture with UN-KC-6141 when the macrophages attained the pro-inflammatory state. This was considered 0th h time point, and the UN-KC-6141 cells were collected at 6, 8, 12, 24, 48 and 72 h of treatment for RNA extraction and apoptosis assay by FACS. Macrophages were collected for RNA extraction. No trace of macrophages was found in the wells, where UN-KC-6141 cells were seeded.

2.16. Orthotopic pancreatic cancer induction and mice treatment

To develop orthotopic pancreatic tumor, UN-KC-6141 pancreatic cancer cells (0.5×10^6 cells/50 μl) were orthotopically injected into the pancreases of C57BL/6 mice. Animals were anesthetized with intraperitoneal administration of a cocktail mixture of ketamine (80 mg/kg) and xylazine (8 mg/kg). After sterilizing the incision site, approximately 1 cm long incision was made in the abdomen near the position of spleen. Gently the pancreas along with the spleen was pulled up to the incision site, and 0.5×10^6 UN-KC-6141 cells in 50 μl volume were injected into the pancreas using a 30-guage needle. After resetting all the pre-moved organs, the abdomen was closed with absorbable catgut sutures. The skin incision was closed with interrupted sutures of non-absorbable material. The skin suture material was removed at approximately five days following the surgical procedure. The animals were monitored daily.

To analyze the effects of probiotics on orthotopic UN-KC-6141 pancreatic cancer model, LBD-ST was orally gavaged to the mice at a c.f.u. of 1×10^9 on day 0. From the same study, one group of mice was given a booster dose of 1×10^9 on day 7. On day 15 all animals were sacrificed, primary tumor weights were measured, and gross necropsy was performed.

2.17. In vitro study on effect of LDB-ST to polarized RAW 264.7 cells

To further understand the effect of LDB-ST on polarize macrophages we first treated unpolarized RAW 264.7 cells with mouse IL4 (Sigma) at the dose of 20 ng/ml for 24 h to make the cells M2 polarized. After this the cells were treated for 1, 6 and 12 h separately with LDB-ST at a dose of 10 MOI. The results of the treatments were analyzed at transcription and protein level by qRT-PCR and ELISA.

2.18. Graphs and statistical analysis

Principal component analysis (PCA), 1-way and 2-way ANOVA were done to calculate the level of significance. The results shown in the graphs are the mean ± SD ($n \geq 3$). All graphs and statistical analysis was done in GraphPad Prism (V5.04, Prism, USA). PCA was done using GeneSpring GX (v12.1, USA).

3. Results

3.1. Effects of LDB-ST on survival of murine macrophage

Murine macrophage cell line RAW 264.7 was treated with probiotic formulation LDB-ST. RAW 264.7 cells challenged with Salmonella (ST′) was taken as a positive control. Probiotic untreated and ST′ unchallenged cells were considered as negative control. Fig. 1A reports percent survival of RAW 264.7 cells at 1, 2, 4, and 6 h following treatment with LDB-ST at MOIs of 0.5, 1, 10 and 100. Results from challenge studies revealed significant cell death starting at 1 h following treatment with ST′. LDB-ST revealed no toxic effect on murine macrophage RAW 264.7 cells up-to MOI 10, which was selected for further *in vitro* studies reported here. Cell viability was, however, compromised at MOI 100 following 6 h treatment with LDB-ST. Cell viability was over 70% at 6 h following LDB-ST treatment at MOI 100.

3.2. Macrophage whole genome expression study

It is important to understand the molecular basis of differential survivability as well as cellular response at the gene expression level. We performed microarray analysis of genome wide transcriptomic profiling by studying changes in gene expression in RAW 264.7 cells following treatment with LDB-ST. Concomitant with our goal we have presented here expression of genes associated with M1 or M2 polarization of macrophages *in vitro* following treatment with probiotic. Anti-inflammatory polarization state inducible genes or genes expressed following anti-inflammatory polarization are shown in Fig. 1B. Time dependent expression values, for Anti-inflammatory genes reported in Fig. 1B, were highest at 1 h following LDB-ST treatment including. *Arg1*, the marker for anti-inflammatory polarization. Fig. 1C reported expression value of the genes that were responsible for inducing pro-inflammatory macrophage polarization. It is observed that most of the genes and their receptors were up-regulated at 6 h following LDB-ST treatment, which includes *Nos2*, a significant marker for pro-inflammatory macrophages. Presence of *Arg1* and Arginase family genes and absence of *Nos2* activity at the 1 h stage suggested that the associated state was similar to that of an anti-inflammatory macrophage polarization. Immune genes showed a consistent pattern, wherein the anti-inflammatory genes were significantly overexpressed at 1 h and quenched at later time point, while the pro-inflammatory genes followed the opposite pattern. In order to find the coherence of expression of associated genes, we performed Principal Component Analysis (PCA).

PCA analysis further confirmed that the pattern of gene expression profile was significantly different at early (1 h) and late (6 h) time points following probiotic treatment (Fig. S1A). All the analysis were done using those group of genes that have significant (p-value < 0.05) fold changes ≥ 1.5. Out of 32,432 probes, that were spotted on the microarray, total of 5760, 5770, 5324 and 6020 genes were significantly ($p < 0.05$) and differentially expressed in untreated (control) cells and at 1 h, 4 h and 6 h following treatment with LDB-ST. A large number of genes, e,g. 1550, 1296, 1077 and 1603, were uniquely expressed in untreated (control) cells and at 1 h, 4 h and 6 h following treatment with LDB-ST as depicted as Venn diagram in Fig. S1B.

The data discussed here have been deposited in NCBI's Gene Expression Omnibus (Edgar, Domrachev, & Lash, 2002) and are accessible through GEO Series accession number GSE98503 and link is provided below:

https://www.ncbi.nlm.nih.gov/geo/query/acc.cgi?token=ylonyscutlenzgx&acc=GSE98503.

To validate time dependent microarray results of macrophage polarization shift following treatment with LDB-ST, we studied transcriptional expression of select pro- and anti-inflammatory marker genes using qRT-PCR and marker protein expression by fluorescence microscopy, FACS and ELISA.

3.3. Kinetics of gene expression by qRT-PCR

Kinetics of transcriptional expression profile, of marker innate immune genes, was studied *in vitro* with RAW 264.7 cells at 1, 2, 4, 6, 8 and 12 h following treatment with LDB-ST at MOI of 10 (Fig. 1D,E). Transcriptional expression values were calculated in terms of fold change of gene expression following treatment with respect to time matched untreated condition. At MOI 10, expression of *Tgfβr1* and *Arg1*,in murine macrophage cells, decreased significantly ($p < 0.05$) in 6 h with the highest expression observed at 1 h following LDB-ST treatment. The transcriptional expression values of genes, *Il1b*, *Il6*, *Il12*, *Tnf* and *Nos2*increased with time and reached the peak expression at 6 h following LDB-ST treatment. In summary, pro-inflammatory genes, in the murine macrophage RAW 264.7, increased their induced expression with a maximum at 6 h while expression of anti-inflammatory genes decreased with time starting with highest expression at 1hfollowing treatment with LDB-ST. The current profile of inflammatory genes, in murine macrophages following treatment with LDB-ST, is different from expression pattern of inflammatory genes in RAW 264.7 when treated with *Lactobacillus acidophilus* (Fig. S2A, B). We validated the current qRT-PCR results by ELISA, fluorescence microscopy and FACS and described below.

3.4. Secretory proteins by ELISA

We validated expression profile of several pro- and anti-inflammatory genes, such as, IL1b, IL6, IL12, TNFα and TGFβ as reported in the preceding section, at protein level by using ELISA following 1, 2, 4 and 6 h treatment with LDB-ST at MOI of 10. Following treatment at different time points, supernatant media were collected to quantify the proteins secreted following treatment of the cells. We calculated fold change of expression for each protein molecule, following treatment of the RAW cells with LDB-ST, by comparing with respective expression value for time matched untreated control. Kinetics of fold change value for each gene is shown in Fig. 1F and 1G. Fig. 1F, by comparing with Fig. 1D, reveals that ELISA corroborated with qRT-PCR results for IL1b, IL6 and IL12. Results from ELISA (Fig. 1F) further supported the transcriptional data TNFα secretion that increases over time with highest expression at 6 h following LDB-ST treatment of murine macrophage cells. Results in Fig. 1G revealed that expression of TGFβ at 1 h post treatment was 6 fold higher compared to untreated time matched control. Expression of TGFβ decreased with time (Fig. 1G). Using ELISA, we confirmed that IL1b, IL6, IL12, TNFα (pro-inflammatory cytokines) were significantly up-regulated following 6 h of treatment compared to the expression values following 1 h of treatment with LDB-ST. TGFβ (representative of anti-inflammation) had higher expression levels following 1 h of treatment but no expression was detected at 6 h post LDB-ST treatment.

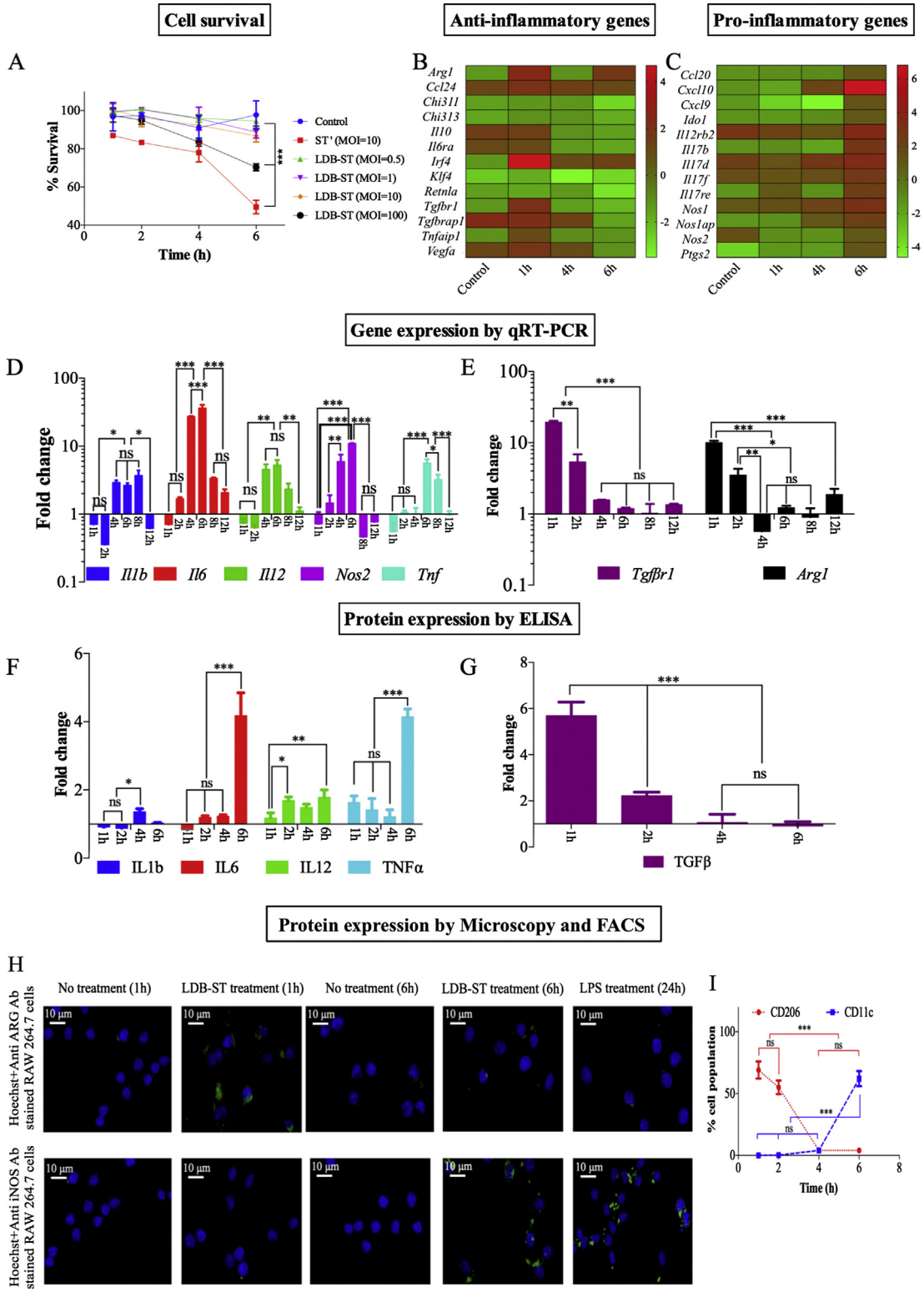

Fig. 1. Survival of, inflammatory responses by and *In vitro* polarization of murine macrophage cell line. (A) Survival of RAW 264.7 cells at various MOIs (0.5, 1, 10 and 100) following treatment with LDB-ST is shown. Survival following challenge with ST′ at MOI 10 is shown as positive control. Expression kinetics of pro- and anti-inflammatory of select innate immune genes in RAW 264.7 cells following treatment with LDB-ST from microarray **(B, C)** and validation by qRT-PCR **(D, E)** are shown. Validation by ELISA for secretory proteins IL1b, IL6, IL12, TNFα (markers for pro-inflammatory macrophage polarization), **(F)** and TGFβ (marker for anti-inflammatory macrophage polarization), **(G)** expression from RAW 264.7 cells following treatment with the LDB-ST at MOI 10. RAW 264.7 cells, treated with LDB-ST at MOI 10 for 1 and 6 h were stained by either fluorescent dye conjugated anti-ARG or anti-iNOS antibody, are shown. Cell nucleus was stained by Hoechst and fluorescence of anti-ARG and anti-iNOS stained RAW 264.7 cells following treatment with LPS are shown as positive control for pro-inflammatory response **(H)**. Graphical representation of the pattern of RAW 264.7 cell population distribution obtained from FACS study for CD11c and CD206 cell surface markers following LDB-ST treatment (MOI 10). Significance levels were calculated using 2-way ANOVA, where n ≥ 3 and significance is denoted by * ($P \leq 0.05$), ** ($P \leq 0.01$), *** ($P \leq 0.001$).

3.5. Marker protein detection through fluorescence microscopy and flow cytometry

NOS2 (or iNOS) and ARG are the polarization markers for macrophages polarized in pro-inflammatory and anti-inflammatory states. Fig. 1H presented the changes in iNOS and ARG expression corroborative of anti- and pro-inflammatory status of RAW 264.7 at 1 h and 6 h post LDB-ST treatment. Results from qRT-PCR for iNOS and ARG were validated by fluorescence microscopy and shown in Fig. 1H. Macrophages following treatment with LDB-ST for 1 h were stained positive with Anti-ARG antibody while treatment with LDB-ST for 6 h were negative for Anti-ARG staining. Similarly, macrophages following treatment with LDB-ST for 1 h were stained negative for Anti-iNOS but were positive with Anti-iNOS antibody staining at 6 h post LDB-ST treatment. Treatment of macrophages with LPS for 24 h, as a positive control for pro-inflammatory response, revealed that macrophages were negative to anti-ARG but were positive to anti-iNOS. To re-confirm time dependent macrophage polarization shift upon LDB-ST treatment, select cell surface markers, CD68, CD11c and CD206, on macrophages were checked by flow cytometry. Macrophage entity and integrity of RAW 264.7 cells were checked with anti CD68 staining (Fig. S3). Fig. S3 depicted that majority of cells in the population are $CD68^+$. CD11c (pro-inflammatory macrophage polarization marker) and mannose receptor CD206 (anti-inflammatory macrophage polarization marker) were also detected on macrophages by flow cytometry following treatment with LDB-ST at MOI 10 in a time dependent manner (Fig. S3). $CD206^+$ macrophages were more at the early time points (69% at 1 h and 57% at 2 h post LDB-ST treatment) and dropped down to 4% at 4 h and 2% at 6 h following treatment with LDB-ST. On the contrary, CD11c population of Macrophages were insignificant until 4 h but become higher (62%) at 6 h following treatment with LDB-ST. No significant $CD11c^+$ cells were detected in untreated time matched control cell population and no significant population of $CD206^+$ cells were recorded for the 4 h and 6 h post probiotic treatment (Fig. 1I).

3.6. M1 Polarization of IL4 treated M2 polarized RAW 264.7 cells in vitro by LDB-ST

We further tested kinetics of expression of *Il10* and *Tnfα* genes at transcriptional level to evaluate the inflammatory status of IL4 treated RAW 264.7 cells following treatment with LDB-ST with respect to IL4 untreated RAW 264.7 cells. Fig. 2A represents the transcriptional expression value of *Il10* and *Tnfα* in murine macrophage cell line RAW 264.7 at 1, 6 and 12 h following treatment with IL4. Fig. 2B further validated the observation at protein level by ELISA. Fig. 2C depicts transcriptional expression of *Il10* and *Tnfα* in IL4 pretreated RAW 264.7 cells at 1, 6 and 12 h following treatment with LDB-ST. Corresponding time matched control data following treatment with LDB-ST in IL4 untreated RAW 264.7 cells are shown in Fig. 2D.

3.7. Gene expression pattern from ex vivo and in vivo studies

Following the observations of macrophage polarization *in vitro* using murine macrophage cell line RAW 264.7, we planned to verify the results *ex vivo* (using primary macrophage cells) and *in vivo* conditions following treatment with LDB-ST. Kinetics of transcriptional expression profile, in terms of fold changes (calculated with respect to expression of genes with respect to time matched untreated controls) of pre-selected innate immune genes, was studied in Th2 and Th1 biased mice. Kinetic profile of gene expression of pro-inflammatory and anti-inflammatory genes was found to follow similar pattern in most cases. *Ex vivo* study suggested, LDB-ST treated primary peritoneal macrophages from BALB/c mice lowered expression of pro-inflammatory genes (like *Il1b*, *Il6*, *Il12* and *Nos2*) at 1 h but started increasing from 6 h to 12 h post treatment with LDB-ST (Fig. 3A). Similar phenomenon was observed with the LDB-ST treated primary cells collected from C57BL/6 mice (Fig. 3B). Anti-inflammatory gene *Tgfβr1* had the highest expression at 1 h following LSB-ST treatment of primary peritoneal macrophages from BALB/c, whereas, *Arg1*was up-regulates following 6 h of LDB-ST treatment (Fig. 3C). No significant changes in *Tgfβr1* gene were observed on LDB-ST treated primary macrophages extracted from C57BL/6, but *Arg1* showed highest expression at 8 h post treatment with LDB-ST (Fig. 3D).

To establish our findings *in vivo* in mice model system, we injected LDB-ST in peritoneum of BALB/c and C57BL/6 mice. Lavage extracted from peritoneum (from BALB/c and C57BL/6 mice) showed highest expression of pro-inflammatory gene (like, *Il1b*, *Il6*, *Il12* and *Nos2*) at 12 h post LDB-ST treatment (Fig. 3E, G). On the other, peritoneal cells from BALB/c and C57BL/6 mice showed the highest expression value of select anti-inflammatory genes (like, *Tgfβr1* and *Arg1*) at 4 h and 6 h, respectively following treatment with LDB-ST (Fig. 3F and H).

We also studied the effects of LDB-ST treatment, on BALB/c and C57BL/6 mice, when treated by oral gavaging. For orally treated mice, we studied the immune bias of the mixed cell population collected from ileum and colon together. Data obtained from orally gavaged BALB/c mice gut tissue samples showed higher *Nos2* expression at 7 days post LDB-ST treatment (Fig. 4A), whereas, *Nos2* expression in C57BL/6 mice was insignificant (Fig. 4C). BALB/c mice, on the contrary, showed higher expression of *Arg1*in intestinal tissue samples on day 1 following oral gavaging and again on day 7 post treatment (Fig. 4B). In C57BL/6 mice, the expression of *Arg1* was initially higher; gradually it gets lowered (Fig. 4D). Remarkably, BALB/c, which is Th2 biased mice, is showing higher *Nos2* expression than Th1 biased C57BL/6 mice.

We also observed the status of peritoneal cells by treating C57BL/6 mice with LDB-ST, orally. Pro-inflammatory genes like *Il1b* and *Nos2* showed its highest expression on day 5 post treatment (Fig. 4E), the expression of *Il6* and *Il12* was found to be around 2 and 3 fold respectively with respect to time matched control. Anti-inflammatory genes *Tgfbr1* and *Arg1* shows maximum 1.9 and 2.2 fold up-regulation on day 1 post LDB-ST gavage (Fig. 4F). As the expression of pro-inflammatory genes started declining 5 days post treatment, we gavaged mice with LDB-ST on day 7 (booster dose) and analyzed gene expression in peritoneal cells. We observed that booster dose was working efficiently, as *Il1b*, *Il6*, *Il12* and *Nos2* showed maximum up-regulation on the next day followed by decrease in expression over next 7 days (Fig. 4G). Noticeably, no anti-inflammatory gene up-regulation was observed (Fig. 4H).

3.8. Effect of LDB-ST activated primary macrophages on UN-KC-6141 cells

Results so far suggested that LDB-ST treatment for longer time can induce pro-inflammatory bias in macrophages. We, therefore, tested the potential of the LDB-ST induced pro-inflammatory biased macrophages to inhibit UN-KC-6141 cell growth. For that we co-cultured LDB-ST activated (to pro-inflammatory state) primary macrophages (collected from C57BL/6 mice) with UN-KC-6141 cells. From FACS study we have found that activated macrophages can induce apoptosis on UN-KC-6141 cells (Fig. 5F-J), where late apoptotic UN-KC-6141 cell population were found to be 21% and 22.5% (Fig. 5K) at 48 h and 72 h respectively. Whereas, no significant change in apoptotic population was observed when un-treated macrophages were co-cultured with UN-KC-6141 cells (Fig. 5A-E). The transcriptional expression level of the extrinsic and intrinsic apoptotic pathway genes was analyzed for UN-KC-6141 upon co-culture with LDB-ST treated peritoneal macrophages from C57BL/6 mice. The genes of extrinsic pathway show a significant up-regulation at 24 h following the co-culture was set (Fig. 5L), while the genes for intrinsic pathway showed almost consistent down-regulation (Fig. 5M). Result from *in vitro* co-culture study suggests, activated macrophages is triggering extrinsic pathway to induce apoptosis onUN-KC-6141 cells.

To further study the plausible cause of apoptotic pathway activation in UN-KC-6141 cells. For that, we analyzed TLR pathway on LDB-ST treated co-cultured primary macrophages (Fig. 5N) and LDB-ST treated

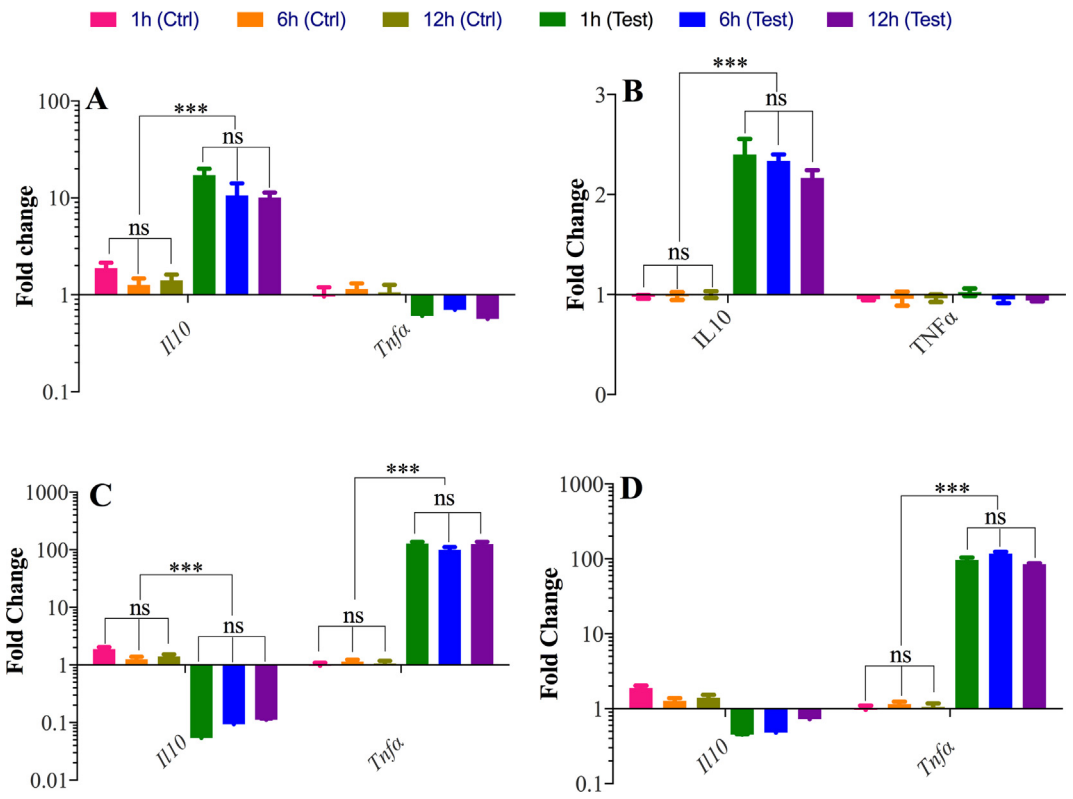

Fig. 2. Effect of LDB-ST on IL4 treated murine macrophage cells. qRT-PCR or transcriptional expression of *Il10* and *Tnfα* in RAW 264.7 cells at 1, 6 and 12 h following treatment with IL4 alone **(A),** IL4 followed by LDB-ST **(C)** and LDB-ST in IL4 untreated cells **(D)**. Protein level expression of IL10 and TNFα in RAW 264.7 cells at 1, 6 and 12 h following treatment with IL4 is shown in Panel **B** for validation. Significance levels were calculated using 2-way ANOVA within ≥ 3 and significance is denoted by *** ($P \leq 0.001$).

primary macrophages (Fig. S4). We have observed that genes which are responsible to trigger TLR pathway went up-regulated 6 h post LDB-ST treatment (Fig. 5N), the expression level of those genes gradually came back to basal level 72 h post LDB-ST treatment.

3.9. Effect of LDB-ST on tumor growth

Iron nanoparticle and genetically engineered *Salmonella typhimurium* have been used to put the TAM in pro-inflammatory state to inhibit tumor growth *in vivo* (Zanganeh et al., 2016; Zheng et al., 2017). With this notion, we went for *in vivo* study with C57BL/6 mice to see whether LDB-ST activated macrophage can coup-up with the tumors induced inside C57BL/6 mice. To understand the efficacy of LDB-ST in orthotopic mice model, UN-KC-6141 cells were injected into the pancreas. The mice group, which was orally gavaged with LDB-ST on day 0 or the group which was given booster dose on day 7 (orally) showed significant reduction in overall tumor weight compared to vehicle treated animals (Fig. 6A). Tumor tissues were analyzed for gene expression where we have found that, the genes like *Tnfr*, *Fadd*, *Casp8*, *Casp7* and *Casp3*, which are responsible to induce apoptosis extrinsically, gets up-regulated in LDB-ST treated mice group (Fig. 6C). Also the reduction of *Arg2* and *Tgfbr1* expression (both in tumor tissue and peritoneal lavage) which are the markers for anti-inflammation was noticed; while a significant increase in *Il1b*, *Il6*, *Il12* and *Nos2* expression (both in tumor tissue and peritoneal lavage) (Fig. 6B, 6D), which are the markers for pro-inflammation, when compared to controls animals.

4. Discussion

Probiotics are well known as innate immune gene modulators in macrophages (Pradhan et al., 2016). Here, a probiotic formulation LDB-ST is tested for their immune modulatory properties *in vitro*, *ex vivo* and *in vivo* system. The results from genome wide microarray analysis, qRT-PCR, ELISA, fluorescence microscopy and FACS have been combined to understand and elucidate the process of immunomodulation following treatment with LDB-ST. Results from *in vitro* studies were validated *ex-vivo* using murine peritoneal macrophages followed by revalidation by *in vivo* studies. Following confirmation of time dependent macrophage polarization, the above said probiotic formulation is used to study tumor growth inhibition in C57BL/6 mice.

Results from microarray studies suggested that genes which are involved to trigger anti-inflammatory response in macrophages went up-regulated 1 h post LDB-ST treatment; whereas, pro-inflammatory response was observed to be maximum at 6 h post LDB-ST treatment on RAW 264.7 cells. Genes involved in oxidative phosphorylation (OXPHOS) (Table S1) had higher expression (e.g. *Atp12* with 7.2 and *Cox10* with 11.2 fold change values) at 6 h of LDB-ST treatment compared to earlier time points for treatment. Arachidonic acid metabolism pathway (shown in Table S2) activity also increased at 6 h in macrophages following treatment with LDB-ST. Arachidonic acid metabolism pathway induces inflammatory leukotrienes and prostanoids, which increase the pro-inflammatory response in macrophages (Funk, 2001). All those supportive pathways re-confirmed the status of pro-inflammatory response at 6 h time point. *In vitro* 4 h time point may simply be during the transition from the anti-inflammatory to pro-inflammatory state; at this time point most of the genes within the glycolytic pathway (shown in Table S3) show down-regulation, of which the detailed status remains unknown.

The genes, validated through qRT-PCR were the major markers for pro-inflammation and anti-inflammation in macrophages. The significant up-regulation of anti-inflammatory genes in the first hour of treatment followed by gradual diminishing of the transcriptional expression levels by sixth hour suggested a shift to a pro-inflammatory or

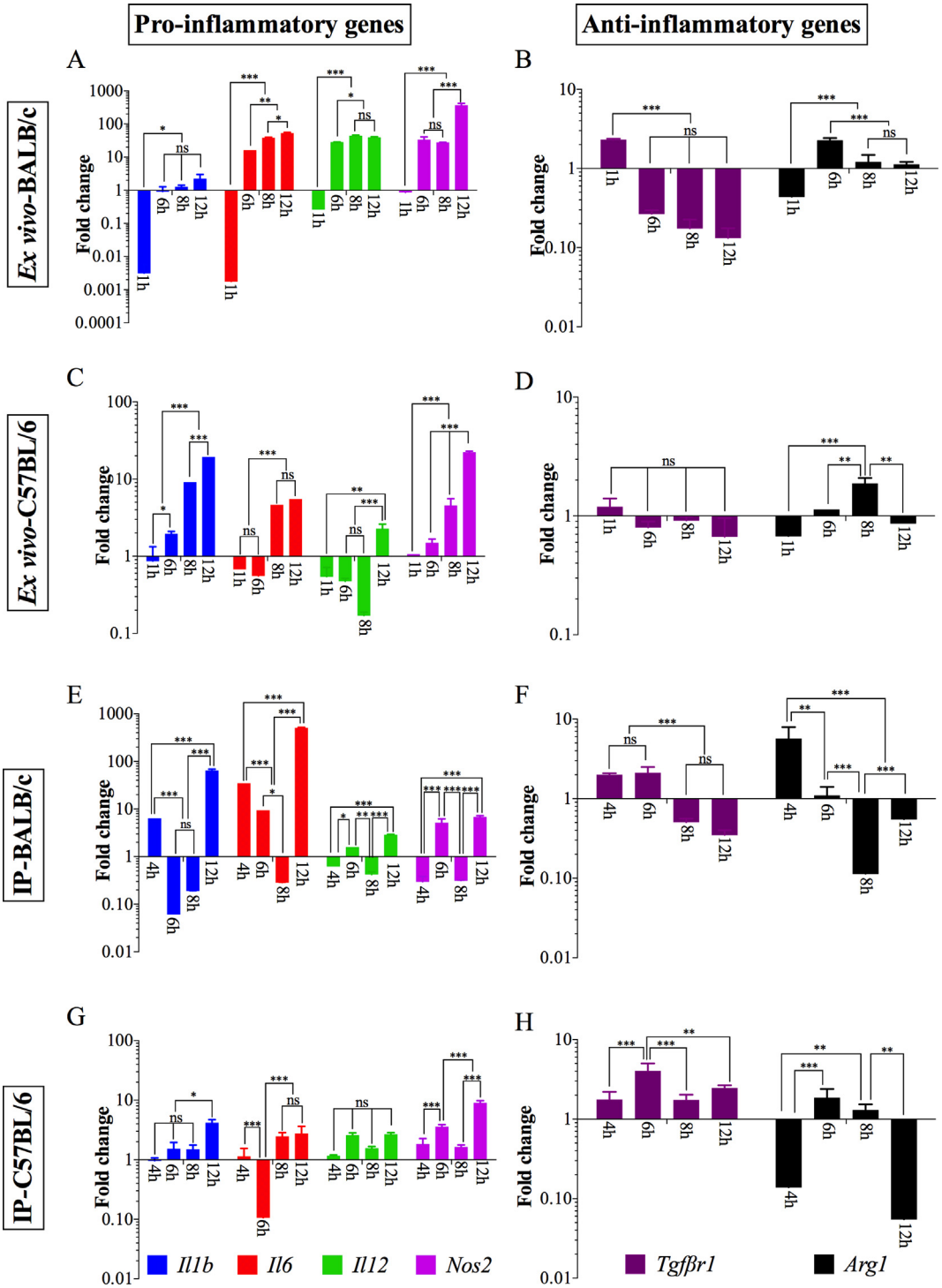

Fig. 3. *Ex vivo* and peritoneal macrophage polarization following treatment with LDB-ST. Effects of treatment with LDB-ST (*ex vivo*) on primary peritoneal macrophages extracted (*ex vivo*) from BALB/c **(A, B)** and C57BL/6 **(C, D)** mice following expressions (fold change w.r.t. untreated time matched control) of pro-inflammatory **(A, C)** and anti-inflammatory **(B, D)** genes are shown. Effects of LDB-ST treatment *in vivo* on peritoneal macrophages extracted from BALB/c **(E, F)** and C57BL/6 **(G, H)** mice following expressions (fold change w.r.t. untreated time matched control) of pro-inflammatory **(E, G)** and anti-inflammatory **(F, H)** genes are shown. Significance levels were calculated using 2-way ANOVA with n ≥ 3 and significance is denoted by * (P ≤ 0.05), ** (P ≤ 0.01), *** (P ≤ 0.001).

pro-inflammatory like state (details in Table 2A–E). This polarization state was confirmed by looking at the protein level using ELISA. Results from Fluorescence microscopic studies re-confirmed anti-inflammatory state of macrophage at 1 h and pro-inflammatory state at 6 h following treatment with LDB-ST at MOI 10. FACS analysis was performed to detect the $CD11c^+$ and $CD206^+$ cell populations, as these are the reliable markers for pro-inflammatory and anti-inflammatory polarized macrophages (Fujisaka et al., 2009). FACS analysis data corroborates previous findings. In addition, we observed that treatment with LDB-ST could also polarize IL4 induced RAW 264.7 cells from M2 to M1 (Fig. 2).

We have tried different combinations to find out how live LDB-ST is different from the others. For that we used heat killed LDB-ST, Lactobacillus acidophilus MTCC-10307 (LA) (a probiotic bacterial

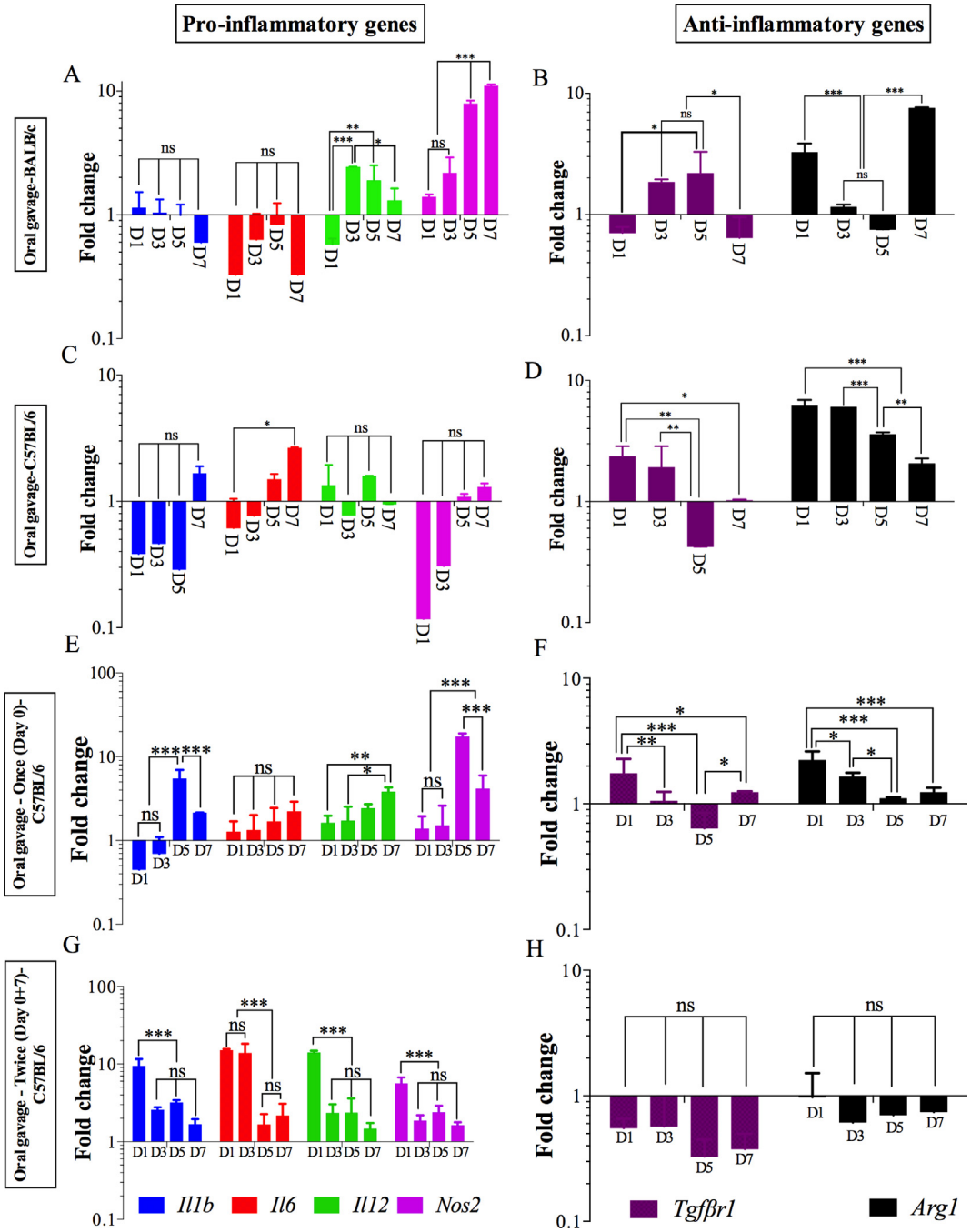

Fig. 4. *In vivo* immune status following treatment with LDB-ST by oral gavaging. Effects of LDB-ST treatment with LDB-ST by oral gavaging once (D0) **(A-F)** or twice (D0 + D7) **(G, H)** in BALB/c **(A, B)** and C57BL/6 **(C-H)** mice by evaluating the expressions of pro-inflammatory and anti-inflammatory genes are shown in gut wall tissues **(A-D)** and on peritoneal macrophages **(E-H)** *in vivo*. Significance levels were calculated using 2-way ANOVA with n ≥ 3 and significance is denoted by * (P ≤ 0.05), ** (P ≤ 0.01), *** (P ≤ 0.001).

strain) and ST′ (*Salmonella typhimurium*, a pathogenic bacteria) with the same protocol. Heat killed LDB-ST treated RAW 264.7 cells showed, up-regulated pro-inflammatory genes (*Il1b*, *Il12* and *Il6*) expression at 4 h of treatment. The anti-inflammatory genes *Tgfbr1* and *Arg1* showed a slow growth to maxima at 4 h (Fig. S5). Following LA treatment, pro-inflammatory genes *Il1b* and *Il6* showed a huge down regulation throughout the whole 12 h of the experiment, while *Il12* started with a very low expression and achieved a peak at 4 h, which again came down by the end of 12 h. Expression of *Nos2* showed a minimum at 4 h and eventually achieved a small maximum at 12 h (Fig. S2A). The anti-inflammatory genes *Tgfbr1* and *Arg1* showed same pattern as that of *Nos2* but with insignificant expression (Fig. S2B). Following ST′ treatment, the cells exhibited a strong up-regulation of pro-inflammatory *Il1b* gene at the early time point (1 h post treatment). The genes *Il1b*, *Il6* and *Nos2* showed up-regulated expression at 8 h of treatment which came down by 12 h of treatment (Fig. S2C). The anti-inflammatory genes *Tgfbr1* and *Arg1* showed a constant down-regulation throughout (Fig. S2D). From this set of experiments, it is clear how LDB-ST is different from the others. With this conclusive evidence, that LDB-ST is different from the others, we went ahead with our study using live LDB-ST to understand its efficacy on *ex vivo* and *in vivo* model.

Ex vivo study with peritoneal macrophages extracted from BALB/c or C57BL/6 shows same pattern of macrophage polarization. The *ex vivo* treatment of murine macrophage at MOI 10, for both BALB/c and

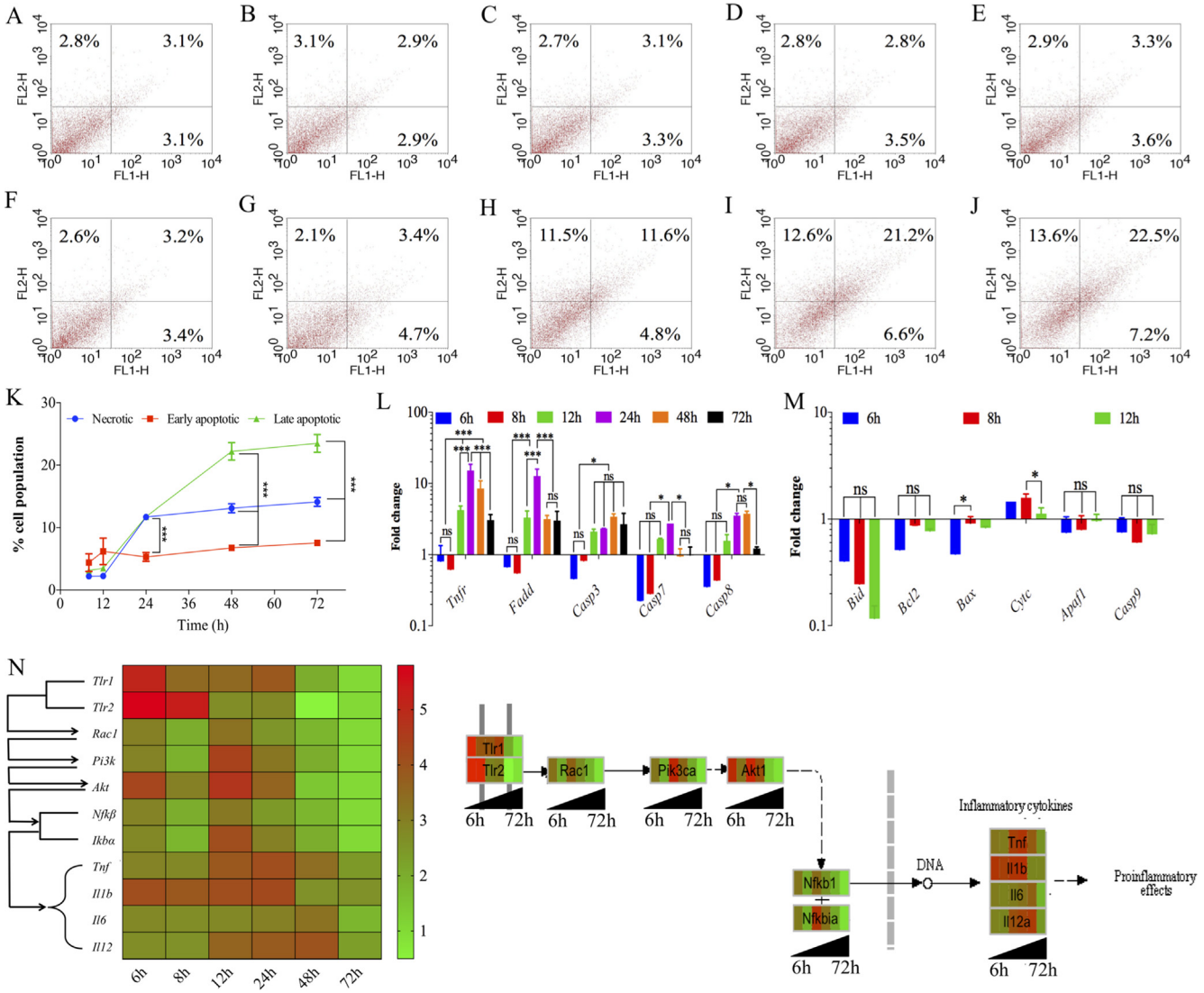

Fig. 5. Effect of activated primary macrophages on UN-KC-6141 cells. Dot plot from FACS analysis **(A-J)** shows the population distribution of normal (PI^--$FITC^-$, lower left quadrant), necrotic (PI^+, upper left quadrant), early apoptotic ($FITC^+$, lower right quadrant) and late apoptotic (PI^+-$FITC^+$, upper right quadrant) cells. UN-KC-6141 cell population distribution is shown when co-cultured with un-treated **(A-E)** or LDB-ST activated **(F-J)** primary macrophages for 8 h **(A, F)**, 12 h **(B, G)**, 24 h **(C, H)**, 48 h **(D, I)** and 72 h **(E, J)**; distribution of cell population from FACS assay is shown graphically **(K)**. Genes responsible to trigger apoptosis (in UN-KC-6141 cells when co-cultured with activated primary macrophages) through extrinsic **(L)** and intrinsic **(M)** pathway is shown. TLR pathway inside activated macrophages during co-culture with UN-KC-6141 cells for different time point is shown through heat-map **(N)**. Significance levels were calculated using 2-way ANOVA with n ≥ 3 and significance is denoted by * ($P \leq 0.05$), ** ($P \leq 0.01$), *** ($P \leq 0.001$).

C57BL/6 showed very specific temporal modulation of the marker immune gene for anti-inflammatory and pro-inflammatory, *Arg1* and *Nos2* respectively. This result was further corroborated by the gene expression pattern of peritoneal macrophages from intra-peritoneally treated and orally gavaged mice, giving a clear polarization trend where moderate pro-inflammation is prominent in later time points. Notably, the current study is reporting for the first time an unusual time dependent immune-modulatory property of probiotic bacteria.

After having confirmation of LDB-ST induced macrophage polarization from *in vitro*, *ex vivo* and *in vivo* studies, we went on to look at effectiveness of the probiotic LDB-ST on tumor growth inhibition. We found that co-culture of LDB-ST activated pro-inflammatory macrophages with UN-KC-6141 cells can trigger extrinsic pathway of apoptosis and eventually cause apoptosis in UN-KC-6141 cells. It has already been reported that, LPO, which are known to induce pro-inflammatory response in macrophages can induce apoptosis in THP-1 cells (Aliprantis et al., 1999). Results from ELISA assay suggested that RAW 264.7 cells releases TNFα on 6 h post LDB-ST treatment. TNFα is known to induce extrinsic pathway mediated cell death in tumor cells (Fulda & Debatin, 2006). The effect of *Lactobacillus plantarum*, a potential probiotic, to combat against colorectal cancer by inducing caspase-mediated apoptosis is well documented (Hendler & Zhang, 2018). The expression of genes *Fadd* and *Casp8* also hints towards a possible involvement of FAS pathway for apoptosis induction. Significant down-regulation of *Bcl2* and *Casp9* shows a definitive lack of intrinsic pathway mediated apoptosis (Kuwana & Newmeyer, 2003).

5. Conclusions

Till date, several studies have shown the immune modulatory effects of different probiotic bacteria in RAW 264.7 cells, the consensus from most of these studies were an immune priming that included a moderate pro-inflammatory expression of genes could reduce the cytotoxicity of the cells following challenge with pathogens (Peña et al., 2005; Pradhan et al., 2016). Several studies had been executed to understand early time point inflammation in RAW 264.7 following pathogen

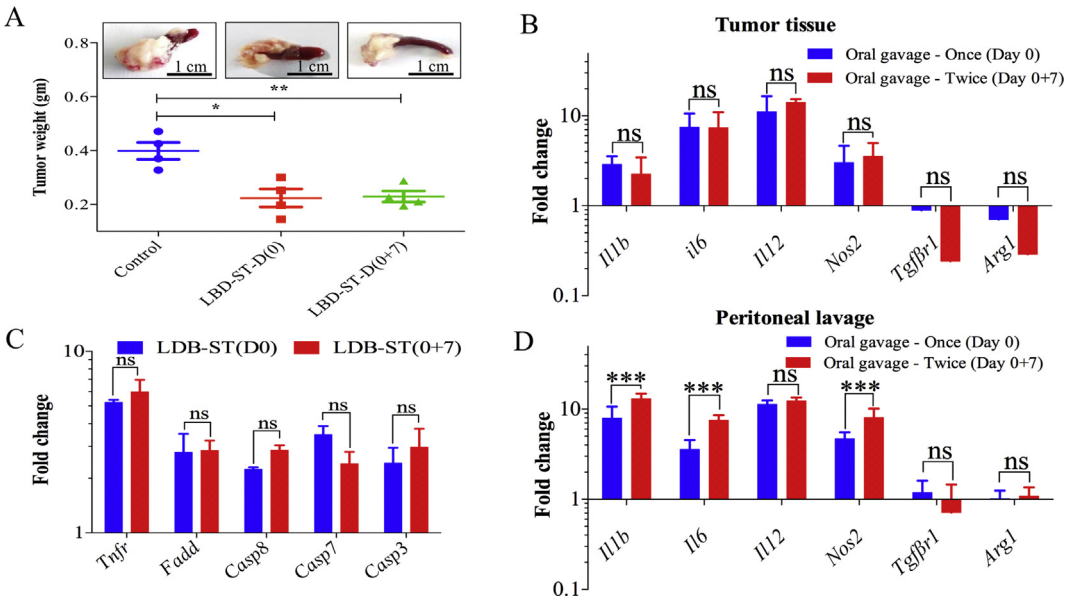

Fig. 6. Effect of LDB-ST on induced tumor inC57BL/6 mice. Effect of LDB-ST on pancreatic tumor mass (orthotopically induced by injecting UN-KC-6141 cells) **(A)**, status of apoptotic **(C)** and immune genes **(B, D)** in tumor tissue **(B)** and peritoneal lavage **(D)** is shown. Significance levels were calculated using 2-way ANOVA with n ≥ 3 and significance is denoted by * (P ≤ 0.05), ** (P ≤ 0.01), *** (P ≤ 0.001).

Table 2A
Comparative expression of immune genes in murine macrophage cell line Raw 26 following treatment with LDB-ST or IL4.

Genes	Fold Change													
	LDB-ST treated RAW 264.7								IL4 treated RAW 264.7				IL4+LDB-ST treated	
	qRT				ELISA				qRT		ELISA		qRT	
	1h	2h	4h	6h	1h	2h	4h	6h	1h	6h	1h	6h	1h	6h
Il1b	↓	↓↓	↑↑	↑↑	↓	↓	↑	↓						
Il6	↓	↑	↑↑↑↑	↑↑↑↑	↓	↑	↑	↑↑↑↑						
Il12	↓	↓	↑↑↑	↑↑↑	↑	↑↑	↑↑	↑↑						
Tnf	↓			↑↑↑↑	↑	↑	↑	↑↑↑↑	↓↓	↓↓	↓↓	↓↓	↑↑↑↑	↑↑↑↑
Il10	↓↓			↓↓					↑↑↑↑	↑↑↑↑	↑↑↑↑	↑↑↑↑	↓↓↓	↓↓↓
Tgf*βr1*	↑↑↑↑	↑↑↑	↑	↑	↑↑↑	↑↑	—	—						
Arg1	↑↑↑↑	↑↑	↓	↑										
Nos2	↓	↑	↑↑↑	↑↑↑										
CD206					↑↑	↑↑	—	—						
CD11c					—	—	—	↑↑						

Table 2B
Comparative expression of immune genes in primary peritoneal macrophages following treatment with LDB-ST.

Genes	LDB-ST treated primary macrophages *(ex vivo)*								LDB-ST treated primary macrophages (*in vivo*)							
	BALB/c				C57BL/6				BALB/c				C57BL/6			
	1 h	6 h	8 h	12 h	1 h	6 h	8 h	12 h	1 h	6 h	8 h	12 h	1 h	6 h	8 h	12 h
Il1b	↓↓↓↓	—	↑	↑↑	—	↑↑	↑↑↑	↑↑↑↑	↑↑↑	↓↓↓	↓↓	↑↑↑↑	—	↑	↑	↑↑
Il6	↓↓↓↓	↑↑	↑↑↑	↑↑↑↑	↓	↓↓	↑↑↑	↑↑↑	↑↑↑	↑↑	↓	↑↑↑↑	—	↓↓↓	↑↑	↑↑
Il12	↓	↑↑↑	↑↑↑	↑↑↑	↓	↓↓	↓↓↓	↑↑	↓	↑	↓	↑↑	↑	↑↑	↑↑	↑↑
Nos2	—	↑↑↑	↑↑↑	↑↑↑↑	—	↑↑	↑↑↑	↑↑↑↑	↓↓	↑↑	↓↓	↑↑	↑	↑↑	↑	↑↑↑
Tgf*β*	↑↑	↓↓↓	↓↓↓	↓↓↓	↑	↓	↓	↓	↑↑	↑↑	↓↓	↓↓	↑↑	↑↑↑	↑↑	↑↑
Arg1	↓↓	↑↑	↑	↑	↓	↑	↑↑	↓	↑↑↑	—	↓↓↓	↓	↓↓↓	↑↑	↑	↓↓↓↓

infection. It is the elevated inflammation that leads to cell death (Bröker, Kruyt, & Giaccone, 2005). We decided to test the efficacy of LDB-ST in tumor growth. It is well established that tumor micro-environment is populated with anti-inflammatory macrophages, which allows tumor to grow efficiently (Chanmee et al., 2014). But, forcefully manipulation of TAM (to pro-inflammatory) is proved to be beneficial in tumor reduction (Zanganeh et al., 2016; Zheng et al., 2017). Current results affirmed that LDB-ST could decrease tumor growth by polarizing TAM to pro-inflammatory state. Genes, responsible to trigger apoptosis through extrinsic pathway, were also up-regulated. Current findings may hold immense potential to inhibit tumor progression via promoting pro-inflammatory tumor associated macrophages (Fig. S6). The current

Table 2C
Comparative expression of immune genes in gut tissue and peritoneal macrophages following treatment with LDB-ST *in vivo*.

Genes	LDB-ST treated gut tissue *(oral gavage)*								LDB-ST treated peritoneal macrophage *(C57BL/6)*							
	BALB/c				C57BL/6				Oral gavage once				Oral gavage twice			
	D1	D3	D5	D7	D1	D3	D5	D7	D1	D3	D5	D7	D1	D3	D5	D7
Il1b	–	–	–	↓↓	↓↓↓	↓↓↓	↓↓↓	↑↑	↓↓	↓	↑↑↑	↑	↑↑↑	↑↑	↑↑	↑
Il6	↓↓↓	↓↓	↓	↓↓↓	↓↓	↓	↑↑	↑↑↑	↑	↑	↑	↑↑	↑↑↑↑	↑↑↑↑	↑↑	↑
Il12	↓	↑↑	↑↑	↑	↑	↓	↑	–	↑	↑	↑↑	↑↑↑	↑↑↑↑	↑↑	↑↑	↑
Nos2	↑	↑↑	↑↑↑↑	↑↑↑↑	↓↓↓↓	↓↓↓	↑	↑	↑	↑	↑↑↑↑	↑↑↑	↑↑↑	↑↑	↑↑	↑
Tgfβ	↓	↑↑	↑↑	↓	↑↑	↑↑	↓↓	–	↑↑	–	↓	↑	↓	↓	↓↓	↓↓
Arg1	↑↑↑	↑	↓	↑↑↑↑	↑↑↑↑	↑↑↑↑	↑↑↑	↑↑	↑↑↑	↑↑	↑	↑	–	↓	↓	↓

Table 2D
Comparative expression of genes associated with apoptosis in UN-KC cells and in tumor tissue following treatment with LDB-ST.

Genes	UN-KC-6141 cells						Tumor tissue	
	6 h	8 h	12 h	24 h	48 h	72 h	Gavaged once	Gavaged twice
Tnfr	↓	↓	↑↑↑	↑↑↑↑	↑↑↑↑	↑↑↑	↑↑↑↑	↑↑↑↑
Fadd	↓	↓	↑↑↑	↑↑↑↑	↑↑↑	↑↑↑	↑↑↑	↑↑↑
Casp3	↓↓	↓	↑↑	↑↑	↑↑↑	↑↑↑	↑↑↑	↑↑↑
Casp7	↓↓↓	↓↓↓	↑	↑↑	–	–	↑↑↑	↑↑↑
Casp8	↓↓	↓↓	↑	↑↑↑	↑↑↑	↑	↑↑↑	↑↑↑

Table 2E
Comparative expression at a glance of immune genes in pancreatic tumor tissue following gavage of LDB-ST cocktail.

Genes	Pancreatic tumor tissue		Peritoneal lavage	
	Gavaged once	Gavaged twice	↑↑	↑↑
Il1b	↑↑	↑↑	↑↑	↑↑
Il6	↑↑↑	↑↑↑	↑↑	↑↑
Il12	↑↑↑↑	↑↑↑↑	↑↑↑	↑↑↑
Nos2	↑↑	↑↑	↑↑	↑↑
Tgfβ	–	↓↓	–	–
Arg1	↓	↓↓	–	–

study elucidates the significance of macrophage polarization (from M2 to M1) as a potential mechanism behind LDB-ST mediated antitumor effect *in vivo*, but the effect of this probiotic formulation on other stromal cells cannot be ruled out, which warrants further investigation. The current study revealed that the antitumor activity of the probiotic cocktail LDB-ST is mediated through immune modulation via transition of macrophages from M2 to M1. A summary table (Table 2A–E) is given highlighting the potential of LDB-ST in treating tumor *in vivo*.

Ethics statement

All experiments involving mice were approved by the Institute Animal Ethics committee of NISER as per the guidelines of CPCSEA (Committee for the Purpose of Control And Supervision of Experiments on Animals).

Acknowledgements

Authors acknowledge the facility and infrastructure provided by NISER Bhubaneswar to execute the work. Authors would also like to acknowledge ILS Bhubaneswar for the provision of FACS. All the experiments involving UN-KC-6141 cell line and LDB-ST probiotics were done under the direct supervision of SS and PA.

Author contribution

DG and AB initiated the experiments and analysis of the data related to *in vitro*, *ex vivo* and *in vivo* studies however DG continued to complete the study and draft the current manuscript. RM added the results corresponding to Fig. 2. BRP assisted in designing and performing microarray experiments. MP and GA provided LDB-ST. DG, AB, SSB and SBS conducted *in vivo* tumor experiments. PA conceptualized, supervised, analyzed and finalized the work and the manuscript.

Funding

This research did not receive any specific grant from funding agencies in the public, commercial, or not-for-profit sectors.

Conflict of Interest

Authors declare no conflict of Interest.

Appendix A. Supplementary material

Supplementary data to this article can be found online at https://doi.org/10.1016/j.jff.2019.03.030.

References

Aliprantis, A. O., Yang, R.-B., Mark, M. R., Suggett, S., Devaux, B., Radolf, J. D., ... Zychlinsky, A. (1999). Cell activation and apoptosis by bacterial lipoproteins through toll-like receptor-2. *Science, 285*(5428), 736–739.
Bröker, L. E., Kruyt, F. A. E., & Giaccone, G. (2005). Cell death independent of caspases: A review. *Clinical Cancer Research, 11*(9), 3155–3162.
Carper, J. (1994). *Food-your miracle medicine.* Harper Collins.
Chanmee, T., Ontong, P., Konno, K., & Itano, N. (2014). Tumor-associated macrophages as major players in the tumor microenvironment. *Cancers, 6*(3), 1670–1690.
Dean, M., Fojo, T., & Bates, S. (2005). Tumour stem cells and drug resistance. *Nature Reviews Cancer, 5*(4), 275.
Dinarello, C. A. (2000). Proinflammatory cytokines. *Chest Journal, 118*(2), 503–508.
Driessen, F. M., Kingma, F., & Stadhouders, J. (1982). Evidence that Lactobacillus bulgaricus in yogurt is stimulated by carbon dioxide produced by Streptococcus thermophilus. *Netherlands Milk and Dairy Journal (Netherlands)*.
Edgar, R., Domrachev, M., & Lash, A. E. (2002). Gene Expression Omnibus: NCBI gene expression and hybridization array data repository. *Nucleic Acids Research, 30*(1), 207–210.
Fujisaka, S., Usui, I., Bukhari, A., Ikutani, M., Oya, T., Kanatani, Y., ... Urakaze, M. (2009). Regulatory mechanisms for adipose tissue M1 and M2 macrophages in diet-induced obese mice. *Diabetes, 58*(11), 2574–2582.
Fulda, S., & Debatin, K.-M. (2006). Extrinsic versus intrinsic apoptosis pathways in anticancer chemotherapy. *Oncogene, 25*(34), 4798.
Funk, C. D. (2001). Prostaglandins and leukotrienes: Advances in eicosanoid biology. *Science, 294*(5548), 1871–1875.
Gordon, S. (2003). Alternative activation of macrophages. *Nature reviews immunology, 3*(1), 23–35.
Guha, D., Bhowmik, S., & Ghosh, R. (2014). Influence of ultraviolet C bystander effect on inflammatory response in A375 cell on subsequent exposure to ultraviolet C or hydrogen peroxide. 51, 552–558.
Hendler, R., & Zhang, Y. (2018). Probiotics in the treatment of colorectal cancer. *Medicines (Basel), 5*(3), 101.
Herve-Jimenez, L., Guillouard, I., Guedon, E., Boudebbouze, S., Hols, P., Monnet, V., ... Rul, F. (2009). Postgenomic analysis of streptococcus thermophilus cocultivated in

milk with Lactobacillus delbrueckii subsp. bulgaricus: Involvement of nitrogen, purine, and iron metabolism. *Applied and Environment Microbiology, 75*(7), 2062–2073. https://doi.org/10.1128/AEM.01984-08.
Knox, S. J., & Meredith, R. F. (2000). Clinical Radioimmunotherapy.
Kuwana, T., & Newmeyer, D. D. (2003). Bcl-2-family proteins and the role of mitochondria in apoptosis. *Current Opinion in Cell Biology, 15*(6), 691–699.
Lamagna, C., Aurrand-Lions, M., & Imhof, B. A. (2006). Dual role of macrophages in tumor growth and angiogenesis. *Journal of Leukocyte Biology, 80*(4), 705.
Lawrence, T., & Natoli, G. (2011). Transcriptional regulation of macrophage polarization: Enabling diversity with identity. *Nature Reviews Immunology, 11*(11), 750–761.
Lyke, K. E., Burges, R., Cissoko, Y., Sangare, L., Dao, M., Diarra, I., ... Doumbo, O. K. (2004). Serum levels of the proinflammatory cytokines interleukin-1 beta (IL-1β), IL-6, IL-8, IL-10, tumor necrosis factor alpha, and IL-12 (p70) in Malian children with severe Plasmodium falciparum malaria and matched uncomplicated malaria or healthy controls. *Infection and Immunity, 72*(10), 5630–5637.
Mantovani, A., Allavena, P., Sica, A., & Balkwill, F. (2008). Cancer-related inflammation. *Nature, 454*(7203), 436.
Mantovani, A., Biswas, S. K., Galdiero, M. R., Sica, A., & Locati, M. (2011). Macrophage plasticity and polarization in tissue repair and remodelling. *The Journal of Pathology, 229*(2), 176–185.
Mantovani, A., Sozzani, S., Locati, M., Allavena, P., & Sica, A. (2002). Macrophage polarization: Tumor-associated macrophages as a paradigm for polarized M2 mononuclear phagocytes. *Trends in Immunology, 23*(11), 549–555.
Martinez, F. O., & Gordon, S. (2014). The M1 and M2 paradigm of macrophage activation: Time for reassessment. *F1000Prime Reports, 6*(13.10), 12703.
Milenic, D. E., Brady, E. D., & Brechbiel, M. W. (2004). Antibody-targeted radiation cancer therapy. *Nature Reviews Drug Discovery, 3*(6), 488.
Mosser, D. M., & Edwards, J. P. (2008). Exploring the full spectrum of macrophage activation. *Nature Reviews Immunology, 8*(12), 958.
Peña, J. A., Rogers, A. B., Ge, Z., Ng, V., Li, S. Y., Fox, J. G., & Versalovic, J. (2005). Probiotic Lactobacillus spp. diminish Helicobacter hepaticus-induced inflammatory bowel disease in interleukin-10-deficient mice. *Infection and Immunity, 73*(2), 912–920.
Pradhan, B., Guha, D., Ray, P., Das, D., & Aich, P. (2016). Comparative analysis of the effects of two probiotic bacterial strains on metabolism and innate immunity in the RAW 264.7 murine macrophage cell line. *Probiotics and Antimicrobial Proteins, 8*(2), 73–84.
Ray, A., & Dittel, B. N. (2010). Isolation of mouse peritoneal cavity cells. *JoVE (Journal of Visualized Experiments), 35* e1488–e1488.
Reid, G., Jass, J., Sebulsky, M. T., & McCormick, J. K. (2003). Potential uses of probiotics in clinical practice. *Clinical Microbiology Reviews, 16*(4), 658–672.
Solinas, G., Germano, G., Mantovani, A., & Allavena, P. (2009). Tumor-associated macrophages (TAM) as major players of the cancer-related inflammation. *Journal of Leukocyte Biology, 86*(5), 1065–1073.
Torres, M. P., Rachagani, S., Souchek, J. J., Mallya, K., Johansson, S. L., & Batra, S. K. (2013). Novel pancreatic cancer cell lines derived from genetically engineered mouse models of spontaneous pancreatic adenocarcinoma: Applications in diagnosis and therapy. *PLoS One, 8*(11), e80580.
Van Cutsem, E., Köhne, C.-H., Hitre, E., Zaluski, J., Chang Chien, C.-R., Makhson, A., ... Bodoky, G. (2009). Cetuximab and chemotherapy as initial treatment for metastatic colorectal cancer. *New England Journal of Medicine, 360*(14), 1408–1417.
Veringa, H. A., Galesloo, T. E., & Davelaar, H. (1968). Symbiosis in yoghurt. 2. Isolation and identification of a growth factor for Lactobacillus bulgaricus produced by streptococcus thermophilus. *Netherlands Milk and Dairy Journal-Nederlands-Nederlands Melk en Zuiveltijdschrift, 22*(3), 114.
Vinogradov, S., Warren, G., & Wei, X. (2014). Macrophages associated with tumors as potential targets and therapeutic intermediates. *Nanomedicine, 9*(5), 695–707.
Wang, N., Liang, H., & Zen, K. (2014). Molecular mechanisms that influence the macrophage m1â€“m2 polarization balance. *M1/M2 Macrophages: The Arginine Fork in the Road to Health and Disease, 230*.
Xie, L., Ortega, M. T., Mora, S., & Chapes, S. K. (2010). Interactive changes between macrophages and adipocytes. *Clinical and Vaccine Immunology, 17*(4), 651–659.
Zanganeh, S., Hutter, G., Spitler, R., Lenkov, O., Mahmoudi, M., Shaw, A., ... Moseley, M. (2016). Iron oxide nanoparticles inhibit tumour growth by inducing pro-inflammatory macrophage polarization in tumour tissues. *Nature Nanotechnology, 11*(11), 986.
Zheng, J. H., Nguyen, V. H., Jiang, S.-N., Park, S.-H., Tan, W., Hong, S. H., ... Bom, H.-S. (2017). Two-step enhanced cancer immunotherapy with engineered Salmonella typhimurium secreting heterologous flagellin. *Science Translational Medicine, 9*(376), eaak9537.